

Research Paper

Salinity Effects on Anionic AEC Surfactant with n-Decane: IFT, Phase Behavior, Solubilization, Microemulsion Viscosity

Boni Swadesi*, Fadhlan Barrul Azmi, Avianto Kabul Pratiknyo, Aditya Kurniawan, Suwardi Universitas Pembangunan Nasional Veteran Yogyakarta, Indonesia

Revised: Oct 6, 2025 Received: Sept 30, 2025 Accepted: Oct 6, 2025 Online: October 14, 2025

Abstract

n-Decane is a common model oil for isolating salinity effects in surfactant systems. In anionic AEC formulations, salinity influences IFT reduction, microemulsion topology, solubilization capacity, and flow behavior. The objectives of this study were to evaluate the effect of NaCl salinity (0-32,000 ppm) on IFT, Winsor transitions, solubilization ratio, and microemulsion viscosity in n-decane/AEC systems, and to determine working concentrations using a CMC test derived from IFT. In this study, the method used was to determine the CMC from the breakpoint of the IFT curve versus the log concentration of AEC in the reference brine. Working concentrations of 2 percent w/w. were selected above the CMC. IFT was measured with a spinning-drop tensiometer at a controlled temperature. Phase behavior was mapped through a salinity scan to identify Winsor I-III-II. The solubilization ratio was calculated from the volume of the middle phase at equilibrium composition. The viscosity of the microemulsion was characterized using a Brookfield DV3T (C40 spindle) with a stepwise shear protocol. In n-decane model systems, salinity governs interfacial properties and phase structure that, in turn, modulate rheology. CMC-by-IFT selection of working dose and tuning salinity near HLD 0 provide a reliable framework for AEC formulation design and for calibrating process parameters ahead of controlled core-flood studies.

Keywords: Salinity, Phase Behavior, Solubilization Ratio, Microemulsion Viscosity, EOR

INTRODUCTION

Enhanced Oil Recovery (EOR) continues to play a critical role in maximizing hydrocarbon recovery from mature reservoirs, where primary and secondary recovery methods have reached their economic limits. Among various EOR methods, chemical flooding using surfactants has attracted increasing attention due to its ability to reduce oil-water interfacial tension (IFT), alter rock wettability, and mobilize residual oil trapped in the pore spaces. Anionic surfactants are particularly favorable because of their strong surface activity, chemical stability, and relatively low cost. However, their performance is highly sensitive to salinity and ionic composition of the reservoir brine, which can influence micellization, adsorption, and microemulsion behavior. Therefore, understanding the relationship between salinity and surfactant efficiency is crucial to designing formulations that perform reliably under reservoir conditions.

n-Decane is widely used as a model oil to isolate and evaluate the physicochemical behavior of surfactant systems under controlled laboratory conditions. In the case of anionic AEC surfactants, variations in salinity affect not only IFT reduction but also microemulsion phase behavior, solubilization ratios, and rheological properties, factors that directly influence oil recovery efficiency. Mapping these interdependencies enables the identification of the optimal salinity range near the hydrophilic-lipophilic deviation (HLD \approx 0), where the surfactant achieves the most balanced affinity between the aqueous and oil phases. Accordingly, this study investigates the effect of NaCl salinity on the interfacial and rheological behavior of AEC surfactant systems with n-decane,

Copyright Holder:

providing a scientific foundation for subsequent formulation optimization and core-flood validation.

Despite extensive cEOR research with complex crude oils, fewer studies have mapped in detail how salinity governs the coupled responses of AEC-n-decane systems, including IFT reduction, explicit Winsor transitions, solubilization capacity, and microemulsion viscosity. Such integration is critical for translating molecular and interfacial insights into macroscopic design rules for laboratory flooding and eventual field application. Therefore, the objective of this study is to systematically investigate the effect of NaCl salinity (0–32,000 ppm) on IFT, phase behavior, solubilization ratio, and microemulsion viscosity in AEC-n-decane formulations, while establishing a practical workflow that combines CMC-by-IFT determination with salinity tuning near HLD ≈ 0 for robust formulation design.

LITERATURE REVIEW

n-Decane is widely employed as a model oil to decouple reservoir-fluid compositional complexity and isolate the fundamental roles of surfactant chemistry and brine composition in chemical enhanced oil recovery (cEOR) (Jafari Pour et al., 2024; Mehrabianfar et al., 2021). In surfactant flooding, interfacial tension (IFT) reduction, wettability adjustment, and microemulsion formation are leveraged to mobilize residual oil otherwise trapped by capillary forces and unfavorable viscous-interfacial force balances (Rotelli et al., 2017; Schoeling et al., 1989; Sheng, 2013). Using a single-component oil such as n-decane enables controlled interrogation of these mechanisms and facilitates quantitative mapping between formulation variables and interfacial or flow responses (Isaac et al., 2022; Rosen, 1989; Schramm & Kutay, 2010). Among anionic surfactants (Al-Badi et al., 2022; Kopanichuk et al., 2022; Scerbacova et al., 2022), alkyl ethoxy carboxylates (AEC) have attracted interest for their ability to achieve ultra-low IFT in saline environments while maintaining acceptable electrolyte and thermal tolerance; industrial routes for AEC production are established and documented (Rosen, 1989; Schramm & Kutay, 2010). When appropriately formulated with brine, AEC systems can yield a middle-phase (Winsor III) microemulsion in which the surfactant partitions are comparable between oil and water phases. This balanced state is closely associated with HLD ≈ 0 (hydrophilic-lipophilic deviation) and is frequently accompanied by minimum IFT, high solubilization ratios, and distinctive rheology. Salinity is the principal lever steering interfacial thermodynamics toward or away from HLD ≈ 0 . Increasing ionic strength screens electrostatic interactions, modifies head-group hydration (saltingout), and alters preferred interfacial curvature, thereby driving transitions across Winsor I-III-II regions (Rosen & Kunjappu, 2012; Schramm & Kutay, 2010; Sheng, 2013). The magnitude and direction of these shifts depend on the oil's hydrophobicity, often parameterized by its equivalent alkyl carbon number (EACN). Relative to typical light crudes (e.g., effective EACN \approx 8–9), n-decane possesses a higher effective EACN, so formulations commonly require higher salinity to reach the balanced Winsor III region and ultra-low IFT (Rosen, 1989; Schramm & Kutay, 2010).

Beyond interfacial thermodynamics, microemulsion viscosity is pivotal for mobility control. Near-optimal salinity, microemulsions often display shear-thinning and exhibit a maximum viscosity close to $HLD \approx 0$, which can improve mobility ratio and sweep efficiency; however, excessive viscosity may elevate injection pressures and exacerbate heterogeneity (Jin et al., 2023; Massarweh & Abushaikha, 2020; Rosen, 1989; Schramm & Kutay, 2010). Thus, establishing the coupling between salinity, microstructure, and rheology is essential to balance injectivity with displacement efficiency in practice (Jin et al., 2023; Massarweh & Abushaikha, 2020; Schramm & Kutay, 2010; Taber et al., 1997). A rigorous formulation workflow begins by setting the working surfactant concentration via a CMC-by-IFT screening: plotting IFT versus the logarithm of AEC concentration in a reference brine reveals a breakpoint interpreted as the critical micelle

concentration (CMC) (Al-Soufi & Novo, 2021; Perinelli et al., 2020). Working doses are then selected above the CMC to ensure sufficient interfacial aggregation for sustained IFT reduction and robust microemulsion formation before salinity optimization (Massarweh & Abushaikha, 2020; Rosen, 1989; Schramm & Kutay, 2010; Sheng, 2013). This staged approach, first fixing concentration, then sweeping salinity, reduces confounding and supports reproducible comparisons across tests (Rotelli et al., 2017; Schoeling et al., 1989; Sheng, 2013; Taber et al., 1997b).

Despite extensive precedent on cEOR with complex crudes, fewer studies present an integrated and quantitative map linking salinity to (i) ultra-low IFT, (ii) explicit Winsor transitions, (iii) solubilization ratio from equilibrium middle-phase volumes, and (iv) microemulsion viscosity for AEC-n-decane systems. Such integration is valuable because it spans scales, from interfacial partitioning and curvature control to macroscopic flow behavior, thereby reducing uncertainty in selecting operating salinity and surfactant dosage for coreflooding and, ultimately, field application (Isaac et al., 2022; Massarweh & Abushaikha, 2020; Rosen, 1989; Schramm & Kutay, 2010; Sheng, 2013; Taber et al., 1997a). Accordingly, this work investigates NaCl salinity from 0 to 32,000 ppm in an AEC-n-decane system to: (1) delineate the salinity window that yields ultra-low IFT and a balanced Winsor III microemulsion; (2) relate that optimum to peaks in solubilization ratio and characteristic rheology; and (3) articulate a practical design rule that combines CMC-by-IFT selection of working concentration with targeting HLD ≈ 0 for salinity. The resulting framework is intended to guide brine selection, slug sizing and sequencing, and adaptive injection strategies, and to provide a reproducible laboratory foundation for translating formulation insights to controlled coreflood experiments and, ultimately, field-scale implementation (Isaac et al., 2022; Massarweh & Abushaikha, 2020; Rosen, 1989; Schoeling et al., 1989; Schramm & Kutay, 2010; Sheng, 2013; Taber et al., 1997b).

RESEARCH METHOD

Material

The oil phase was n-decane. The aqueous phase used synthetic NaCl brines prepared at prescribed salinities. The surfactant was an anionic Alkyl Ethoxy Carboxylate (AEC). Deionized water (Aqua DM) and analytical-grade NaCl were used for all solutions. Key instruments included an Anton Paar DMA 4100M densimeter, a TX-500D spinning-drop tensiometer, a Brookfield DV3T rheometer with cone-plate spindle CPE-40, and a thermostated water bath/oven.

Preparation of Synthetic Brines and Surfactant Solutions

Brines were prepared at salinities of 0, 500, 1,000, 2,000, 4,000, 8,000, 16,000, 24,000, and 32,000 ppm by weighing NaCl, adding water to target mass/volume, and stirring to homogeneity. Surfactant stock/working solutions (0.5-3.0 % w/w) were prepared by mass and magnetic stirring until homogeneous.

Experimental Design

Unless noted, all tests were conducted at $60\,^{\circ}\text{C}$ to emulate reservoir temperature. The main salinity sweep covered 0–32,000 ppm, with working surfactant levels subsequently fixed from the CMC–IFT screen.

Density Measurements

Fluid densities (aqueous and oil phases) were measured prior to IFT tests with the Anton Paar 4100M following the stepwise procedure: instrument calibration and temperature setting, injection of \sim 3 mL sample without bubbles, and recording the reading. Density differences were then used as inputs for spinning-drop calculations.

Interfacial Tension (IFT) and CMC Determination

IFT was measured with a TX-500D spinning-drop tensiometer. A capillary tube was filled with ~20 mL test brine/surfactant solution; a 2 μ L crude-oil droplet was introduced; the tube was sealed, mounted, and equilibrated at the temperature. The software was configured (video input, ruler/orthogonal measurement), rotation set to 3000 rpm, images acquired every 120 s for 30 min, and drop dimensions recorded to compute IFT at equilibrium.

A CMC–IFT screening at 16,000 ppm salinity (60 °C, 3000 rpm) was performed across 0– 3.0~% w/w AEC to identify the breakpoint where further concentration increases did not significantly lower IFT. These results were used to lock the working concentrations for subsequent tests.

1. Aqueous Stability

Aqueous stability was assessed by storing 15 mL aliquots of surfactant solution in sealed test tubes at room temperature and at $60~^{\circ}\text{C}$ (oven) for seven days, with daily visual documentation of phase changes.

2. Phase Behavior (Salinity Scan) and Solubilization Ratios
For phase behavior, equal volumes of crude oil and surfactant solution (1:1) were loaded
into 5 mL flame-sealed tubes, agitated to mix, and aged at 60 °C for seven days. Phases
(upper/middle/bottom) were recorded daily using the salinity-scan, from which oil- and
water-solubilization ratios (Vo/Vs, Vw/Vs) and phase type (Winsor I/III/II) were
determined.

3. Microemulsion Viscosity

Microemulsion viscosity was measured using a Brookfield DV3T rheometer (cone-plate CPE-40) following the instrument setup and test-configuration steps (leveling, AutoZero, speed programming, spindle selection, temperature control with water bath). Shear-rate/torque data were collected under stepped-shear. For data interpretation, a power-law model ($\tau = K \cdot \gamma^n$) was fit to stress-rate data to classify fluid behavior (n < 1: shear-thinning; n = 1: Newtonian; n > 1: shear-thickening). For non-Newtonian samples, the reported viscosity corresponds to $\gamma = 7 \text{ s}^{-1}$ as a reservoir-representative rate. The testing sequence can be seen at Figure 1.

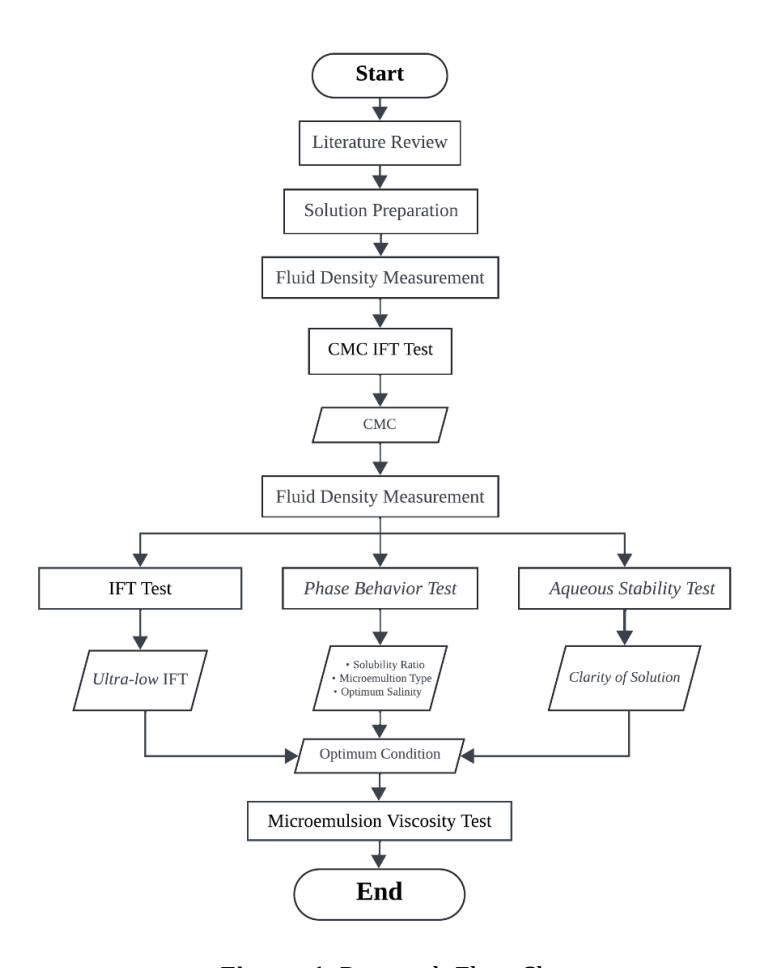


Figure 1. Research Flow Chart

FINDINGS AND DISCUSSION Critical Micelle Concentration (CMC)

Critical micelle concentration (CMC) was screened via interfacial-tension measurements to identify the threshold beyond which additional AEC no longer appreciably reduced IFT. Measurements were made using a TX-500D spinning-drop tensiometer at 60 °C and 3000 rpm in 16,000 ppm NaCl brine. The CMC obtained under these conditions was subsequently adopted as the fixed surfactant dosage for all later experiments. For n-decane, as shown in Figure 2, the IFT decreased steadily over the initial concentration range and then leveled off, indicating diminishing interfacial gains before the onset of micellization. A pronounced drop to the low-IFT band ($\approx 10^{-2}$ dyne/cm) occurred at 2.0 % w/w, after which further concentration increases did not yield additional IFT reduction. On this basis, the CMC under the stated conditions is taken as 2.0 % w/w.

From a physicochemical perspective, the threshold marks a shift from an adsorption-limited regime, where added surfactant chiefly occupies the oil–water boundary, to a bulk, micelle-controlled regime. As interfacial sites near saturation, additional molecules yield only negligible decreases in interfacial free energy; consequently, the IFT reaches a plateau and may exhibit a modest upturn above the CMC. This mechanistic interpretation is consistent with established adsorption–micellization frameworks and matches the biphasic IFT-concentration response observed for the n-decane system.

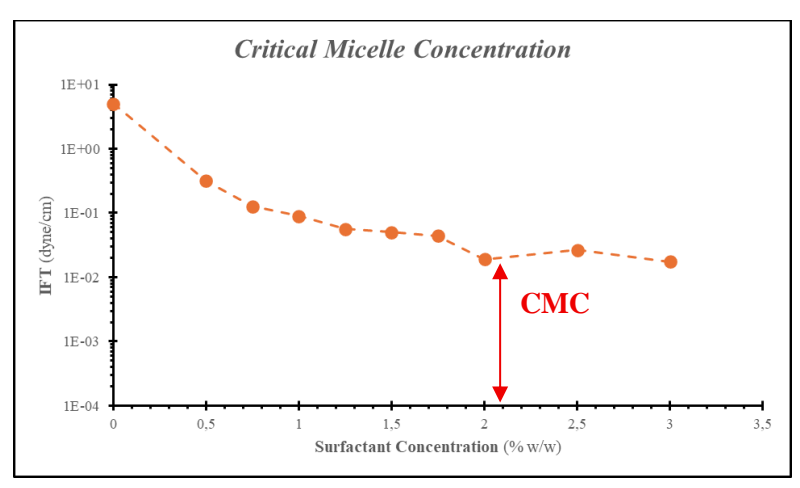
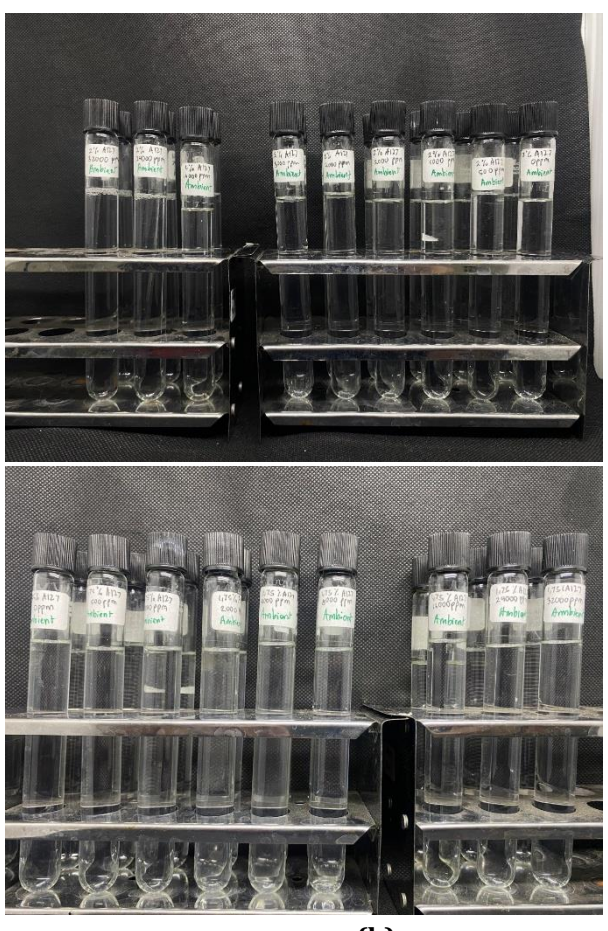


Figure 2. Critical Micelle Concentration

Aqueous Stability Analysis

We evaluated the aqueous-phase compatibility of the AEC system in NaCl synthetic brines using a 7-day hold test at two temperatures, ambient laboratory conditions and 60 $^{\circ}$ C (reservoir analogue). As detailed in the Methods, aliquots at the target salinities were dispensed into 15 mL vials, sealed, and placed either on the bench or in a 60 $^{\circ}$ C oven. Samples were inspected daily for turbidity, visible solids, or macroscopic layering. Recording procedures and pass/fail thresholds matched the study-wide documentation and criteria.



(a) (b)

Figure 3. Documentation aqueous stability test at ambient temperature for 2 %w/w EAC with salinity variations, (a) Day-0, (b) Day-7

At the operating dosage established from the CMC assessment (2% w/w), the AEC solution remained optically clear across the full NaCl salinity window (0-32,000 ppm) during the seven-day room-temperature hold (Figure 3). Daily inspections showed no visible sediment, creaming, or macroscopic phase splitting. Taken together, these observations indicate strong brine compatibility, with high aqueous solubility of the surfactant and a uniformly dispersed continuous phase maintained for the entire test period.

An equivalent qualitative response was obtained at 60 °C: across the entire salinity series, samples remained optically clear for the full seven-day hold (Figure 4), with no haze, gelation, or macroscopic phase splitting. The lack of heat-induced cloud points indicates that the AEC maintains effective hydration of its ethoxy-carboxylate headgroup and resists salt-promoted association, implying robust colloidal stability and minimal electrolyte-driven micellar growth under the thermal conditions evaluated.

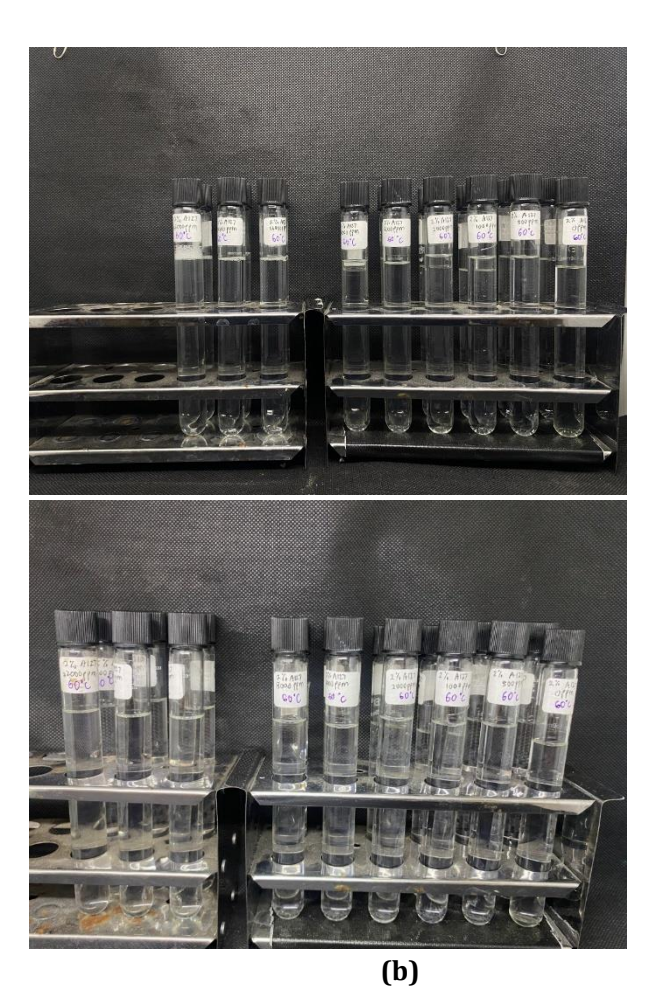


Figure 4. Documentation aqueous stability test at temperature 60°C for 2 %w/w EAC with salinity variations, (a) Day-0, (b) Day-7

(a)

IFT Analysis

Figure 5 depicts the response of interfacial tension (IFT) to NaCl salinity for the AEC/n-decane system at the working concentration fixed from the n-decane CMC screen, using an identical spinning-drop protocol (60 °C, 3000 rpm, equilibrium capture) to ensure methodological continuity.

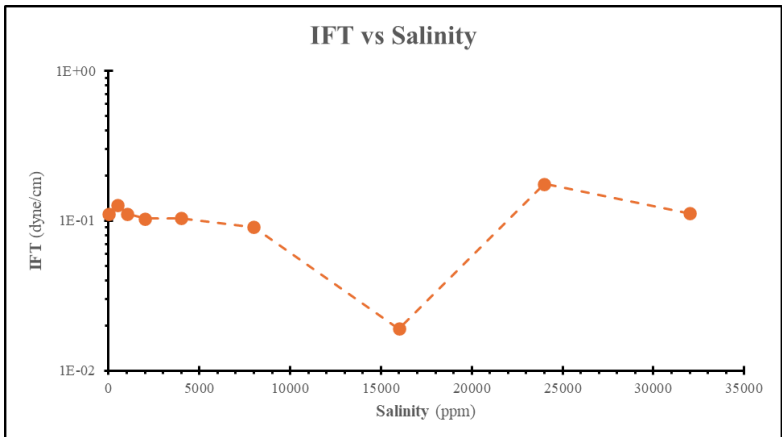


Figure 5. IFT vs Salinity on n-decane

Quantitatively, the IFT-salinity curve is non-monotonic. Starting at 0 ppm, IFT is in the 10^{-1} dyne/cm band (1.11×10^{-1} dyne/cm), rises slightly at 500 ppm (1.28×10^{-1} dyne/cm), and then decreases gradually through 1,000–8,000 ppm ($1.11 \times 10^{-1} \rightarrow 9.05 \times 10^{-2}$ dyne/cm). A distinct minimum occurs at 16,000 ppm with IFT of 1.90×10^{-2} dyne/cm, after which the curve rebounds at higher salinity (24,000 ppm: 1.75×10^{-1} dyne/cm; 32,000 ppm: 1.12×10^{-1} dyne/cm). These values delimit a salinity window centered near 16,000 ppm where IFT is lowest for n-decane under the present conditions.

The trend aligns with salinity-controlled interfacial thermodynamics. At low-moderate ionic strengths, compression of the electrical double layer and partial dehydration of the ethoxy-carboxylate headgroup incrementally improve interfacial packing, but the system remains away from balance; the sharper collapse at 8,000-16,000 ppm reflects an approach toward a more favorable hydrophilic-lipophilic condition (HLD \rightarrow 0) and denser interfacial adsorption. Beyond the minimum, progressive salting-out and increasing effective lipophilicity shift the system away from balance, explaining the IFT rebound at 24,000-32,000 ppm.

In summary, the n-decane data establish a salinity-dependent IFT profile with a clear minimum at 16,000 ppm, bounded on the low-salinity side by modest decreases from 0–8,000 ppm and on the high-salinity side by a rebound attributable to electrolyte-driven lipophilic shifts. This window will be used as the reference for integrating IFT with the phase-behavior and rheology results presented next.

Phase Behavior Analysis

Phase behavior was probed by aging a sealed 1:1 mixture of n-decane and the AEC brine across the salinity grid at $60\,^{\circ}$ C with daily observation, following the same tube protocol used elsewhere in this work. The objective was to identify Winsor regions and, when present, a middle-phase (Type III) microemulsion under reservoir-representative conditions.

At a concentration of 2% w/w AEC, as shown in Figure 6, the system remained lipophilic over the entire salinity range, presenting Winsor II characteristics with no middle-phase (Winsor III) detected. Thus, increasing ionic strength steered the formulation away from the balanced

interfacial state required for a middle phase, consistent with a salting-out-driven shift toward oil-continuous microemulsions.



Figure 6. Documentation of phase behavior test on n-decane with 2% w/w EAC (baseline-0-500-1000-2000-4000-8000-16000-24000-32000 ppm)

Salinity-scan analysis tracked the oil (Vo/Vs) and water (Vw/Vs) in solubilization ratios to diagnose microemulsion balance. For n-decane at 2% w/w, both ratios were relatively flat across the salinity series, and no intersection (Vo/Vs = Vw/Vs) was observed within the tested range, indicating the absence of an optimum salinity defined by balanced solubilization. This outcome is consistent with the persistent Winsor II behavior: the lack of a middle phase suppresses the rise of one solubilization ratio to meet the other, so the balance point does not materialize under these conditions.

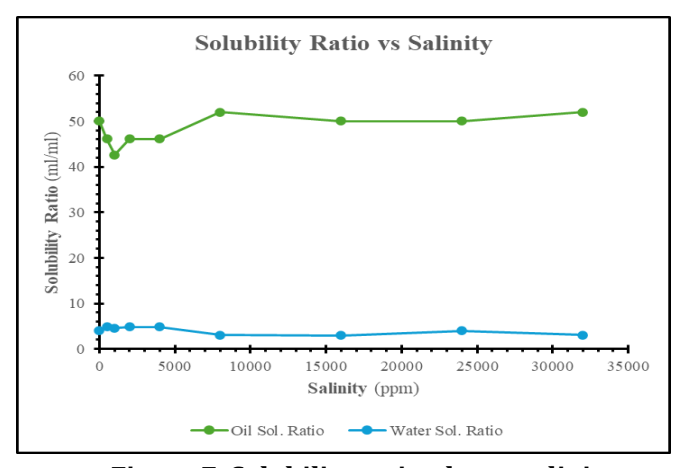


Figure 7. Solubility ratio plot vs salinity

Interpretation. Collectively, the n-decane results show that, at 2% AEC, salinity increases do not induce a balanced (Winsor III) window; instead, the system remains lipophilic with near-constant solubilization ratios, precluding an optimum based on Vo/Vs–Vw/Vs crossing. This aligns with the conceptual criterion that optimum salinity coincides with a middle-phase and equal solubilization of oil and water, conditions not met here.

Microemulsion Viscosity Analysis

Microemulsion viscosity was measured with a Brookfield DV3T (cone–plate CPE-40) under stepped-shear at 60 °C; stress–rate data were fitted to a power-law model ($\tau = K \cdot \gamma^n$) to classify flow behavior. For non-Newtonian samples, the reported "apparent viscosity" corresponds to $\gamma = 7 \text{ s}^{-1}$, providing a reservoir-representative comparison across salinities.

Salinity trend (Figure 8). At 0 ppm NaCl, the n-decane microemulsion shows pronounced shear-thinning (power-law n \approx 0.396), with an apparent viscosity of \approx 156.4 cP. Moving to 24,000 ppm, the microemulsion remains shear-thinning but with a weaker non-Newtonian signature (n \approx 0.517); the apparent viscosity decreases to \approx 140.9 cP. At the highest salinity (32,000 ppm), the rheogram again exhibits shear-thinning, with high low-shear viscosities that decay with increasing shear (e.g., \approx 408 cP at the lowest programmed rate, trending downward at higher rates), consistent with a persistent but progressively less connected microstructure.

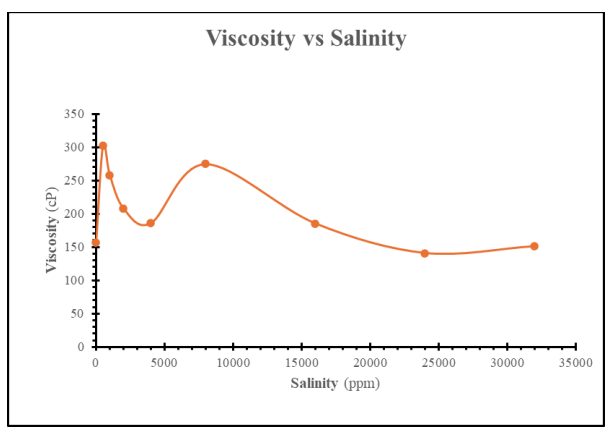


Figure 8. Microemulsion viscosity vs Salinity

The non-monotonic visco-salinity behavior reflects how ionic strength modulates interfacial film packing and inter-micellar connectivity. From 0 to 24,000 ppm, compression of the electrical double layer and partial head-group dehydration diminish film elasticity, reducing microemulsion resistance to shear (drop in viscosity and rise in n toward Newtonian). At very high salinity (32,000 ppm), the rheogram indicates renewed structure at low shear—an effect commonly attributed to salting-out-driven changes in micellar morphology and weak network formation, which produce peaks and troughs in the viscosity landscape across the salinity grid.

As salinity rises, double-layer compression and partial dehydration of ethoxy-carboxylate headgroups diminish interfacial elasticity and reduce the energy penalty for interfacial rearrangements. The practical outcome is a drop in apparent viscosity and an increase in the flow index n (i.e., the system trends closer to Newtonian behavior) over the initial salinity increments.

Beyond a threshold, counterion binding and salting-out shift curvature toward more lipophilic states. Two consequences follow: (i) loss or narrowing of the middle-phase window (transition toward Winsor II/I), which removes bicontinuous network contributions to viscosity; and (ii) under very high salinity, the emergence of weakly connected micellar clusters or elongated aggregates that can rebuild structure at low shear, increasing apparent viscosity only in that regime. This explains why your rheograms show high viscosity at the lowest programmed shear rate at the top-end salinity, while still thinning rapidly as shear increases.

For n-decane at 2 % w/w surfactant, microemulsions persist up to 32,000 ppm and exhibit shear-thinning across all interrogated salinities. The net decrease from \approx 156 cP (0 ppm) to \approx 141 cP (24,000 ppm) at 7 s⁻¹ suggests easing injectivity with increasing ionic strength, while the low-shear build-up at 32,000 ppm cautions that very high salinity can re-introduce microstructural

thickening under gentle shear. These outcomes will be cross-referenced with the salinity-dependent IFT and phase-behavior results to balance mobility control against injectivity in subsequent formulation decisions.

CONCLUSIONS AND FURTHER RESEARCH

This study examines the impact of NaCl salt concentration on the interfacial physics and microstructure of the AEC-n-decane system under conditions representative of reservoir environments. The main conclusions are:

- 1. Working dosage from CMC-IFT. The CMC screen based on the IFT-concentration breakpoint established a defensible working AEC level at 2.0% w/w for the n-decane system; beyond this threshold, additional surfactant did not yield meaningful further IFT reduction. This ensured that subsequent salinity tests probed interfacial effects rather than concentration artifacts.
- 2. Salinity–IFT is non-monotonic with a clear minimum. The IFT–salinity profile showed modest changes from 0–8,000 ppm, a distinct minimum near 16,000 ppm (~1.9×10⁻² dyne·cm⁻¹), and a rebound at higher salinity. Although the minimum was higher than the ultra-low regime typical of light crude, it still represents a functionally significant reduction in interfacial free energy and a practical route to increase capillary number.
- 3. Phase behavior at 2% AEC remained lipophilic. Across 0–32,000 ppm NaCl, the system expressed persistent Winsor II characteristics and no middle-phase (Winsor III) was detected, indicating that the salinity minimizing IFT did not coincide with a balanced microemulsion window for n-decane at this dosage.
- 4. Solubilization ratios did not intersect. Oil and water solubilization ratios remained unbalanced across the grid; Vo/Vs = Vw/Vs was not achieved. Consequently, an "optimum" defined strictly by equal solubilization could not be assigned under the tested conditions, consistent with the absence of a middle phase.
- 5. Shear-thinning rheology with salinity dependence. Where microstructure was present, rheology was shear-thinning over the salinity range interrogated. Apparent viscosity decreased from low to mid-high salinity (easing injectivity), while a low-shear build-up reemerged at the highest salinity—consistent with salt-induced associative structuring. This highlights the need to balance injectivity against any desired mobility control from microstructural thickening.
- 6. Aqueous stability was robust. AEC solutions remained optically clear for seven days at both ambient conditions and 60 °C over 0–32,000 ppm NaCl, supporting reproducible upstream measurements and minimizing risk of precipitation-driven injectivity loss.

This study demonstrates that for n-decane at 2.0% w/w AEC, operating near the IFT minimum (~16,000 ppm NaCl) is effective for capillary desaturation. However, the absence of a stable Winsor III microemulsion window under the tested conditions highlights a key limitation: the system does not naturally achieve balanced phase behavior, which restricts the ability to fully exploit microemulsion-mediated mobility control. This suggests that the formulation, as tested, may be optimal for IFT-driven displacement but less suitable for viscosity enhancement and sweep efficiency under reservoir conditions.

Future studies should therefore refine the formulation by (i) fine-tuning salinity in narrower increments around the IFT minimum, (ii) introducing co-surfactants or co-solvents to broaden the Winsor III region, and (iii) conducting controlled coreflood experiments to directly link laboratory-scale phase behavior with displacement performance. Such follow-up work would provide a more comprehensive understanding of trade-offs between injectivity, stability, and

sweep efficiency, thereby supporting more robust design rules for field-scale application.

ACKNOWLEDGEMENTS

This research was conducted at the Bandung Institute of Technology Energy Building, 7th Floor, Enhanced Oil Recovery (EOR) Laboratory, Faculty of Mining and Petroleum, Jalan Ganesha No.10, Bandung, and funded by LPPM UPN Veteran Yogyakarta.

REFERENCES

- Al-Badi, A., Souayeh, M., Al-Maamari, R. S., & Aoudia, M. (2022). Impact of the molecular structural variation of alkyl ether carboxylate surfactant on IFT reduction and wettability alteration capabilities in carbonates. *Geoenergy Science and Engineering*. https://api.semanticscholar.org/CorpusID:255294739
- Al-Soufi, W., & Novo, M. (2021). A surfactant concentration model for the systematic determination of the critical micellar concentration and the transition width. *Molecules*, *26*(17), 5339. https://doi.org/10.3390/molecules26175339
- Isaac, M. G., Koch, S., & Nefdt, R. (2022). Conceptual engineering: A road map to practice. *Philosophy Compass*, *17*(10), e12879. https://doi.org/10.1111/phc3.12879
- Jafari Pour, M., Manshad, A. K., Zargar, G., & Akbari, M. (2024). Application of alkali-novel green extracted surfactant (AS) for sustainable chemical enhanced oil recovery (CEOR) in carbonate petroleum reservoirs. *Energy & Fuels, 38*(3), 1744–1765. https://doi.org/10.1021/acs.energyfuels.3c03584
- Jin, P., Wu, J., Shi, R., Dai, L., & Li, Y. (2023). Parabolic viscosity behavior of NaCl-thickened surfactant systems upon temperature change. *ACS Omega*, 8(40), 37511–37520. https://doi.org/10.1021/acsomega.3c05855
- Kopanichuk, I. V., Scerbacova, A., Ivanova, A. A., Cheremisin, A. N., & Vishnyakov, A. (2022). The effect of the molecular structure of alkyl ether carboxylate surfactants on the oil-water interfacial tension. *Journal of Molecular Liquids*. https://api.semanticscholar.org/CorpusID:249531333
- Massarweh, O., & Abushaikha, A. S. (2020). The use of surfactants in enhanced oil recovery: A review of recent advances. *Energy Reports*, 6, 3150–3178. https://doi.org/10.1016/j.egyr.2020.11.009
- Mehrabianfar, P., Bahraminejad, H., & Manshad, A. K. (2021). An introductory investigation of a polymeric surfactant from a new natural source in chemical enhanced oil recovery (CEOR). *Journal of Petroleum Science and Engineering,* 198, 108172. https://doi.org/10.1016/j.petrol.2020.108172
- Rosen, M. J. (1989). Surfactants and interfacial phenomena. In Colloids and Surfaces (Vol. 40). https://doi.org/10.1016/0166-6622(89)80030-7
- Rotelli, F., Blunt, M. J., De Simoni, M., Dovera, L., Rotondi, M., & Lamberti, A. (2017). *CO*₂ *injection in carbonate reservoirs: Combining EOR and CO*₂ *storage. OMC 2017 Conference Proceedings* (Paper No. OMC-2017-759).
- Perinelli, D. R., Cespi, M., Lorusso, N., Palmieri, G. F., Bonacucina, G., & Blasi, P. (2020). Surfactant self-assembling and critical micelle concentration: One approach fits all? *Langmuir*, *36*(21), 5745–5753. https://doi.org/10.1021/acs.langmuir.0c00420
- Scerbacova, A., Kopanichuk, I. V., & Cheremisin, A. (2022). Effect of temperature and salinity on interfacial behavior of alkyl ether carboxylate surfactants. *Petroleum Science and Technology,* 41(1), 1–20. https://api.semanticscholar.org/CorpusID:248288221
- Schoeling, L. G., Green, D. W., & Willhite, G. P. (1989). Introducing EOR technology to independent operators. *Journal of Petroleum Technology,* 41(12), 1344–1350. https://doi.org/10.2118/17401-PA

- Schramm, L. L., & Kutay, S. M. (2010). Emulsions and foams in the petroleum industry. In *Surfactants* (pp. 79–118). https://doi.org/10.1017/cbo9780511524844.004
- Sheng, J. J. (2013). Surfactant enhanced oil recovery in carbonate reservoirs. In J. J. Sheng (Ed.), *Enhanced oil recovery field case studies* (pp. 281–299). Gulf Professional Publishing. https://doi.org/10.1016/B978-0-12-386545-8.00012-9
- Taber, J. J., Martin, F. D., & Seright, R. S. (1997a). EOR screening criteria revisited—Part 1: Introduction to screening criteria and enhanced recovery field projects. *SPE Reservoir Engineering*, *12*(3), 189–198. https://doi.org/10.2118/35385-PA
- Taber, J. J., Martin, F. D., & Seright, R. S. (1997b). EOR screening criteria revisited—Part 2: Applications and impact of oil prices. *SPE Reservoir Engineering*, 12(3), 199–206. https://doi.org/10.2118/39234-PA